Biomedicine & Pharmacotherapy 95 (2017) 419–428

Contents lists available at ScienceDirect

Biomedicine & Pharmacotherapy

journal homepage: www.elsevier.com/locate/biopha

Original article

Design and synthesis of conjugated azo-hydrazone analogues using nano $BF_3{\cdot}SiO_2$ targeting ROS homeostasis in oncogenic and vascular progression

Zabiulla[a], V. Vigneshwaran[b], A. Begum Bushra[a], G.S. Pavankumar[b], B.T. Prabhakar[b], Shaukath Ara Khanum[a,*]

[a] Department of Chemistry, Yuvaraja's College (Autonomous), University of Mysore, Mysore, Karnataka, India
[b] Molecular Oncomedicine Laboratory, Postgraduate Department of Studies and Research in Biotechnology, Sahyadri Science College (Autonomous), Kuvempu University, Karnataka, India

ARTICLE INFO

Keywords:
Azo-hydrazone
ROS
Malignancy
Angiogenesis
Dalton's lymphoma ascites tumor

ABSTRACT

Disrupted redox balance is implicated in multiple pathologies including malignant progression and tumor angiogenesis. In this investigation, we report the design and development of novel and effective ROS detoxifying azo-hydrazone molecules targeting malignant pathologies and neoangiogenesis. A series of azo-derivatives conjugated to hydrazones moieties (**9a–j**) were synthesized using Nano $BF_3{\cdot}SiO_2$. The compounds (**9a–j**) were screened for *in-vitro* antioxidant and lipid peroxidation inhibitory activity. Among the series **9a–j**, compound **9f** potently quenched biologically relevant radicals such as superoxide and hydrogen peroxide which emerged as the lead ROS detoxifying molecules. Compound **9f** potently inhibited the proliferative capability of Daltons Lymphoma Ascites (DLA) tumor cells *in-vivo* in dose dependent manner. Regressed tumor progression was correlated with pronounced endogenous antioxidant enzyme superoxide dismutase and catalase *in-vivo*. Also, ROS levels were severely suppressed in **9f** treated mice as assessed by lapsed lipid peroxidation. Altered enzymic and ROS levels *in-vivo* by **9f** were implicated in suppressed VEGF secretion leading to regressed tumor neovasculature and tumor growth. Considering together, it is evident that the synthetic azo-hydrazone analogue **9f** with potent ROS scavenging efficacy inhibits tumor progression and neo-angiogenesis.

1. Introduction

Redox homeostasis is dependent on the delicate balance between the rate and the magnitude of oxidant production and their elimination over time [1]. Oxidative stress generally describes a condition in which cellular antioxidant defence mechanisms are insufficient to inactivate ROS, or excessive ROS are produced, or both. Upregulated ROS levels lead to "non-specific" damage of macromolecules such as DNA, proteins and lipids [2]. This subsequently leads to generation of a new array of oxidation mediated metabolic agents through lipid and protein peroxidation, which are highly destructive than ROS themselves [3]. Growing body of evidence indicates that persistently high ROS levels have been detected in almost all cancers, as a consequence of genetic, metabolic and microenvironment-associated alterations [1]. As a consequence, deregulated redox balance is strongly implicated in multiple aspects of malignant progression and resistance to therapeutic interventions [4]. Tumor growth relies on formation of angiogenesis which is a critical process in the growth, invasion, and metastases of transformed cells. Several lines of recent evidences suggest a pivotal role for ROS signalling in augmenting tumor angiogenesis aiding cancer progression. The reciprocity between oxidative stress and angiogenesis has been centered specifically on the VEGF signalling pathway, engaged in promoting neovasculature [3]. Therefore the phenomenon of ROS-driven cancer progression and angiogenesis has substantially fueled a long-standing interest in the development of effective antioxidant molecules to attenuate neoplastic proliferation through ROS detoxification [4]. Nitrogen-containing compounds are one of the most fruitful and extensively developing fields in chemistry. These compounds display various kinds of biological activities [5–7]. Hydrazones moiety plays an important key role in heterocyclic chemistry [8–13]. It is a class of organic compounds with structure $R_1R_2C = NNH_2$. Hydrazones nucleus exhibited immense pharmacological activities. They are present in many of the bioactive heterocyclic compounds that are of very important use because of their various biological and clinical applications.

Abbreviations: DLA, Daltons lymphoma ascites; VEGF, vascular endothelial growth factor; MVD, microvessel density; TBARS, thiorbarbituric acid reactive substances; DPPH,2, 2 diphenyl-1-picryl-hydrazyl-hydrate; ROS, reactive oxygen species; ELISA, Enzyme linked immunosorbent assay; MDA, malondialdehyde; SOD, superoxide dismutase; H & E, hematoxylin and eosin

* Corresponding author.
E-mail address: shaukathara@yahoo.co.in (S.A. Khanum).

http://dx.doi.org/10.1016/j.biopha.2017.08.076
Received 11 April 2017; Received in revised form 3 August 2017; Accepted 19 August 2017

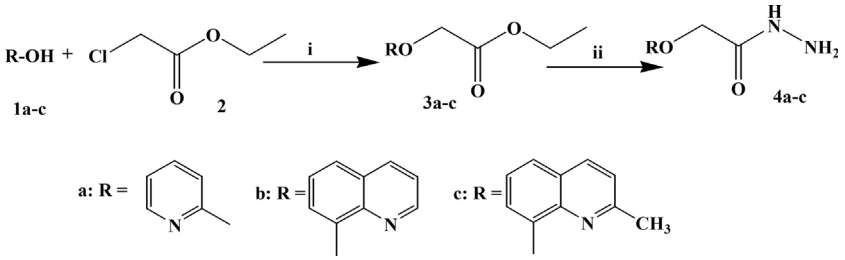

Scheme 1. Synthesis of heteroaryl hydrazide.

(Hetero) aroyl hydrazones demonstrate a wide range of biological activities, including anti-microbial, anti-bacterial, anti-mycobacterial, antifungal, anti-viral, anti-tuberculosis, anti-malarial and anticancer activities [14–21]. On the other hand azo compounds have shown diverse biological activities including antimicrobial antioxidant and antitumor attributes [22–28]. Intrigued to develop a biologically active and potent pharmacophore for oxidant stress and tumor angiogenic pathologies, we in this investigation performed chemical combination of hydrazone and azo compounds to synthesize novel azo-hydrazaide analogous (**9a–j**) using Nano $BF_3{\cdot}SiO_2$. The main objective of this investigation was to select the potent radical quenching azo-hydrazone molecules and analyze its inhibitory effect on *in-vivo* tumor progression and neo-angiogenesis using Dalton's lymphoma murine tumor model.

2. Result and discussion

2.1. Chemistry

The synthesis of the title compounds **9a–j** was accomplished by a synthetic procedure as shown in (Scheme 1–3). All the synthesized compounds were established by IR, proton NMR and mass spectral data. First, the heterocyclic acetic acid ethyl ester **3a–c** were synthesized by the etherification of heterocyclic hydroxyl compounds **1a–c** with chloro ethyl acetate **2** using dry acetone as a solvent to give compounds **3a–c** [7]. The compounds **3a–c** on treatment with 99% hydrazine hydrate yield heteroaryl hydrazide **4a–c** (Scheme 1). The compounds **6a–g** were obtained by refluxing compounds **4a–c** with substituted aromatic aldehydes **5a–d** using ethanol as a solvent. (Scheme 2). Finally, all the substituted benzylidine hydrazone analogous **6a–g**, on treatment with aryl diazonium salt **8a–e** (diazotization of substituted aniline **7a–e** using nano $BF_3{\cdot}SiO_2$ as a catalyst) using sodium hydroxide and ethanol as solvent delivered the expected final products **9a–j** in a good yield. (Scheme 3). All the structures of newly synthesized compounds were assigned on the basis of their spectroscopic data; IR, NMR, LC–MS and C, H, N analysis. The spectra of compounds **4a** was confirmed with the appearance of NH−NH_2 stretching bands at 3100–3205 in IR spectra. In proton NMR, the appearance of two singlet of NH_2 and OCH_2 at δ 4.21 and δ 4.83 respectively and also revealed multiplet signal in the range δ 6.5–7.7 for aromatic protons as well as singlet at 9.5 for NH proton. The mass spectra of compound **4a** gave significant stable M + 1 peak at *m/z* 168 evident the formation of **4a**. Further, a spectrum of the title compound **6a** was considered as a representative example of the series **6a–l.** The IR spectra of the compound **6a** was confirmed by the disappearance of the NH_2 stretching and the appearance 2930 (N−H), 1720 (C=O), 1499 (C=N), 3120–3220 (amide, CO−NH) absorption peaks (cm^{-1}). In addition, ^1H NMR spectra showed disappearance of NH_2 proton and appearance of N=CH protons at δ 8.5, beside increase in aromatic proton with a range of δ 6.5–7.8 and also mass spectra gave significant stable M + 1 peak at *m/z* 270 which clearly affirmed the formation of compound **6a**. The appearance N=N and disappearance NH_2 IR starching of compound **8a** and **7a** respectively, also disappearance of NH_2 proton in NMR its evident for formation of compound **8a**. Finally, in title compounds **9a–l**, compound **9a** taken as a representative example to explain characterizations. The IR spectra was supported by the appearance of N=N stretching band in the IR spectra. Also, the disappearance of N=CH proton, besides, an increase in aromatic protons in the NMR spectra with M + 1 peak at *m/z* at 374 confirmed the product as **9a**.

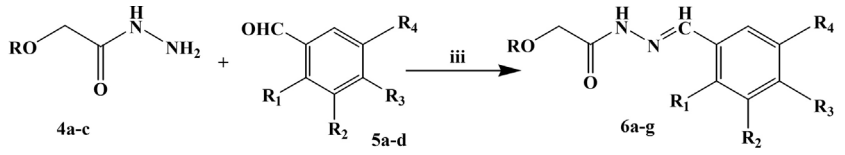

Scheme 2. Synthesis of benzylidene hydrazone analogous.

a:R, R_2, R_3, R_4=H
b:R_1= CH_3, R_2,R_3,R_4=H
c:R_1=OH, R_3=OCH_3,R_2,R_4=H
d:R_1= NO_2, R_4=Cl, R_2, R_3=H

	R			R	
6a	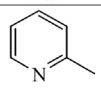	R_1= CH_3, R_2,R_3,R_4=H	6e	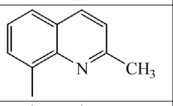	R_1= NO_2, R_4= Cl R_2, R_3 = H
6b		R_1=OH, R_3=OCH_3, R_2,R_4=H	6f	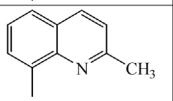	R_1=OH, R_3=OCH_3, R_2,R_4R_5, R_6, R_7=H
6c	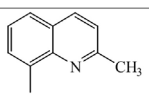	R_1= CH_3, R_2,R_3,R_4=H	6g	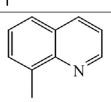	R_1, R_2,R_3,R_4=H
6d	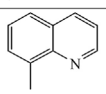	R_1= CH_3, R_2,R_3,R_4=H			

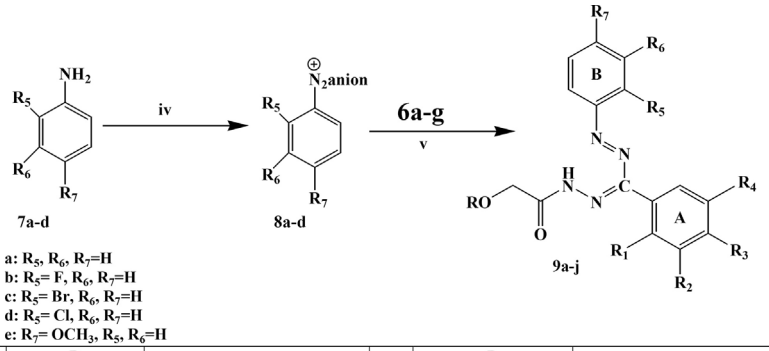

Scheme 3. Synthesis of azo-hydrazone analogues.

	R			R	
9a		R_1= CH_3, R_2,R_3,R_4,R_5, R_6, R_7=H	9f	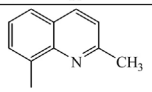	R_1=NO_2, R_4, R_5= Cl R_2,R_3,R_6, R_7=H
9b		R_1=OH, R_3=OCH_3, R_2,$R_4$$R_5$, R_6, R_7=H	9g	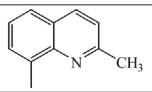	R_1=OH, R_3=OCH_3 R_2,R_4,R_5, R_6, R_7=H
9c		R_1=OH, R_3=OCH_3,R_5= F, R_2,R_4,R_6, R_7=H	9h		R_1=OH, R_3=OCH_3,R_5= Cl R_2,R_4,R_6, R_7=H
9d	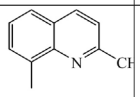	R_1= CH_3,R_5= Br, R_2,R_3,R_4,R_6, R_7=H	9i		R_1= CH_3, R_5= Br, R_2, R_3, R_4, R_6, R_7= H
9e	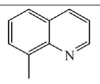	R_1= CH_3, R_2,R_3, R_4,R_5, R_6, R_7= H	9j		R_5= OCH_3, R_1,R_2,R_3,R_4,R_6, R_7=H

2.2. Pharmacology

2.2.1. Compound 9f with inhibitory effect on in-vitro ROS and lipid peroxidation is the lead molecule

Azo and hydrazone compounds were reported to exhibit varied pharmacological activities. The present investigation sought to develop series of novel antioxidant molecules (**9a–j**) by conjugating azo and hydrazine moieties. Preliminarily, the synthesized compounds **9a–j** was subjected to various independent *in-vitro* antioxidant assays. Among the **9a–j** series, compound **9f** potently scavenged the DPPH radical with IC_{50} 9.6 ± 1.15. Then the compounds were investigated for superoxide (O_2^-) and hydrogen peroxide (H_2O_2) scavenging activity, as these reactive oxygen species were associated with various tumorigenic and tumor angiogenesis process [29]. Results demonstrated that similar to DPPH assay, compound **9f** quenched superoxide anion and H_2O_2 radicals with high efficiency with IC_{50} values at 8.56 ± 1.34 and 7.54 ± 1.65 respectively. With respect to the effect on lipid peroxidation, compound **9f** potently inhibited the lipid peroxidation *in-vitro* with IC_{50} 15.6 ± 1.74. Taking together the results elucidate that among the synthesized azo-hydrazone series **9a–j**, compound **9f** displayed the potent ROS scavenging attribute. As ROS is strongly involved in tumor progression and tumor neovasculature, compound **9f** with potent ROS detoxifying potential is opted as the lead molecule for the further anticancer investigation.

2.2.2. Structure activity relationship (SAR) of compound 9f

The azo and hydrazone derivatives are known to be pharmacologically active molecules against various pathological conditions including oxidative stress and malignancy. The current investigation reports the multistep synthesis of conjugated azo-hydrazaide moieties. Structurally, the title compounds are having a basic backbone of one heteroaryl and two aryl rings A and B with azo and imine link and terminal amide group. In order to get the insight into the structure-activity relationship (SAR), we varied the substitutions on both the heteroaryl and aryl rings A and B of these conjugates. Among azo–hydrazone analogues (**9a–j**), compound **9f** displayed potent inhibitory effect on ROS and lipid peroxidation. It is evident from this report that analogue **9f** with both electron withdrawing and electron donating substitution was found to be potent ROS detoxifying and lipid peroxidation inhibitory molecule. Compound **9f** contains 2-nitro and 5-chloro groups in aryl ring A, 2-chloro group in aryl ring B and one methyl group in hetroaryl ring which demonstrated potent ROS quenching attribute and lipid peroxidation inhibition with minimal inhibitory concentration (IC_{50}) as shown in Fig. 1 as verified by DPPH, superoxide anion and H_2O_2 radical scavenging assay. Other tested compounds (**9a–j**) with chloro- and nitro- substitution showed marked radical quenching activity (Fig. 1). Hence this paper provides a novel insight that multi structured azo-hydrazone pharmacophore with electron withdrawing and donating substitution could scavenge biologically relevant radicals involved in malignant pathologies. Finally, considering the IC_{50} values and significant SAR, compound **9f** was selected as the lead molecule for further *in-vivo* antioxidant and tumor angiogenic studies.

2.2.3. Compound 9f regresses DLA tumor progression in-vivo with minimal side effects

The *in-vivo* tumor models are critical for the evaluation of anti-proliferative efficacy. The *in-vivo* anti-proliferative potential of compound **9f** was investigated using a reliable murine Dalton's Lymphoma Ascites (DLA) tumor model. DLA is a widely used cell line to study the *in-vivo* anti-proliferative activity which is known for secretion of ascites fluid containing various growth factors and cytokines for tumor progression [30,31]. Results revealed that administration of compound **9f** at 20 mg/kg *b.w.* concentration exhibited a dose dependent decrease in the tumor development with 83.03% inhibition at the final dose as assessed by the physical morphology (Data not shown) and body weight index (Table 1). The reduced tumorigenic index in **9f** was reflected in the decreased cell density as compared to untreated. As a consequence

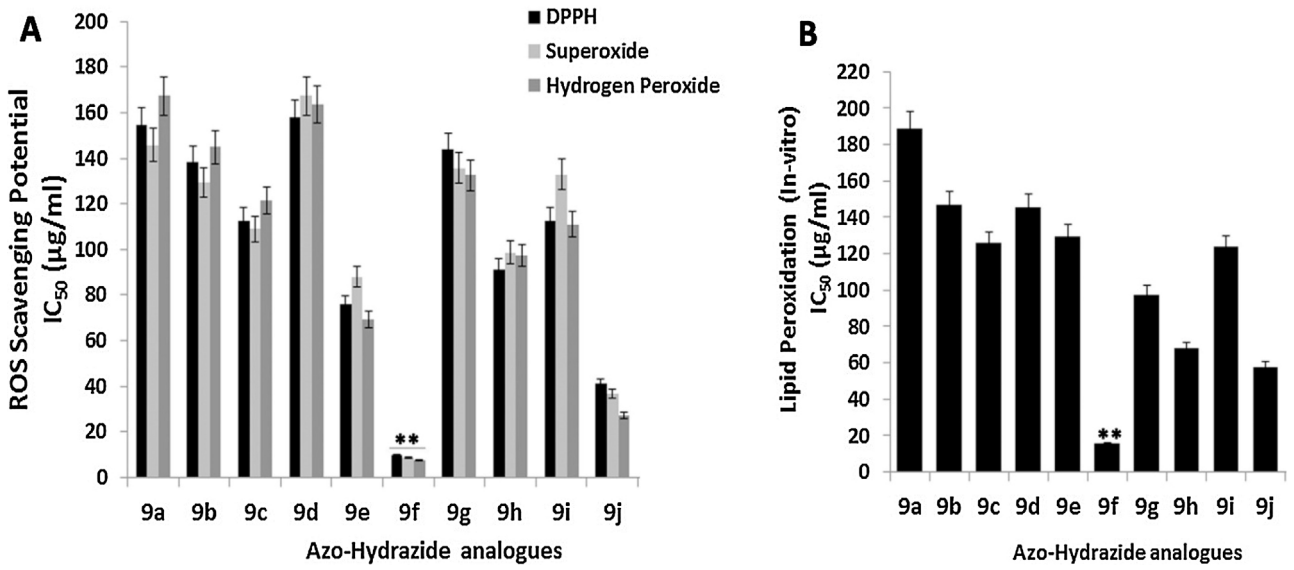

Fig. 1. Screening of potent free radical quenching Azo-Hydrazone analogue from 9a-l series. The IC_{50} of the antioxidant molecules **9a-l** were determined by employing various *in-vitro* radical scavenging and liver lipid peroxidation assays. (A) IC_{50}values of 9a-l series compounds against DPPH, superoxide and hydrogen peroxide radical. (B) Lipid peroxidation inhibitory effect of **9a-l** series *in-vitro*. Peroxidized lipids in liver tissues were estimated by TBARS methods *in-vitro*. By taking IC_{50} values of ROS scavenging potential and lipid peroxidation inhibitory effect, compound **9f** was chosen as the lead molecule. Results are the means of three independent determinations, conducted in triplicate. Statistically significant values are represented as*$p < 0.05$; **$p < 0.01$.

abdominal ascites secretion in the **9f** treated was considerably restrained whereas the control animal depicted abundant secretion (Table 1). As a toxicological assessment, the gross and histopathological appearance of liver and spleen in the **9f** treated DLA animals were analyzed which appeared without any abnormalities as contrary to untreated (Data not shown). Serological and hematological examinations after **9f** treatment in non tumor bearing mice indicated neglible secondary complications (Table 2).

*2.2.4. Compound **9f** inhibits ROS generation by pronouncing ROS neutralizing antioxidant enzymes in-vivo*

ROS poses a significant threat to nucleic acids, proteins, and lipids and, as a result, can lead to a favourable scenario in which oncogenic transformation takes place [32]. Therefore, in order to improve the efficacy of therapeutic agents, strategies which reduce and/or eliminate cellular sources of ROS are needed. So, the anti-proliferative activity of compound **9f** was validated for its implications on ROS and ROS scavenging antioxidant enzyme levels *in-vivo*. ROS levels *in-vivo* was estimated indirectly by measuring the ROS generated secondary oxidative byproducts. ROS reacts with polyunsaturated or poly desaturated fatty acids to initiate lipid peroxidation which generates numerous genotoxic molecules including malondialdehyde (MDA) [2]. Our experimental observation firmly demonstrates that compound **9f** significantly decreased ROS *in-vivo* as evidenced by severely lapsed MDA (Fig. 2A). Furthermore, the cellular redox balance is maintained by powerful antioxidant enzyme system that neutralizes ROS [33]. Among those, the enzymeSuperoxide Dismutases (SODs) that catalyzes the dismutation ofsuperoxide anion radical to oxygen & hydrogen peroxide, and catalase that facilitates the decomposition of hydrogen peroxide to water and oxygen, are pivotal for proper homeostasis [2]. Investigation on the serum enzyme parameters of **9f** treated animal deduced a significantly upregulated SOD and catalase levels *in-vivo* (Fig. 2B & C), in contrast to the untreated mice which paralleled with tumor growth index (Table 1). Altogether, it is clear from this observation that the tumor inhibitory activity of compound **9f** is strongly attributed to its ROS detoxifying behavior.

Table 2
Heamatological and serum parameters of non-tumor normal mice following treatment with compound **9f** at day 10.

S.No.	Hematological and serum parameters	Normal mice	9f treated mice
1.	Alkaline Phosphatase (IU/L)	127.63 ± 2.54	129.62 ± 1.13
2.	Creatinine (mg/dL)	0.62 ± 1.02	0.67 ± 1.53
3.	Urea (mg/dL)	46 ± 2.1	44 ± 1.3
4.	RBC (10^6/µL)	6.86 ± 2.4	6.11 ± 3.6
5.	WBC (10^6/µL)	4.24 ± 2.1	4.7 ± 2.7

Results are the means of three independent determinations, each conducted in triplicate.

2.2.5. Compound 9f attenuates VEGF and tumor neovasculature by modulating ROS

Angiogenesis, the process wherein new blood vessels are formed from pre existing blood vessels, is a critical determinant of cancer growth [32]. DLA tumor growth is related to the progression of

Table 1
Tumor inhibitory effect of azo-hydrazone analogue 9f in Dalton's lymphoma ascites (DLA) tumor model. DLA transplanted mice was administered intraperitoneally with **9f** at 20 mg/kg *b.w.* concentration for three doses and tumor inhibition of the drug was analyzed. Tumor volume was determined by assessing the body weight of **9f** treated mice as compared to control.

S.No	Tumor Parameters	I DOSE		II DOSE		III DOSE	
		Control	9f	Control	9f	Control	9f
1	Tumor volume (g)	6.4 ± 0.6	3.1 ± 0.4	9.2 ± 0.6	2.5 ± 0.3*	12.4 ± 0.5	2.1 ± 0.2**
2	Tumor inhibtion (%)	0	51.6	0	72.83	0	83.07
3	Ascites Secretion (mL)	6.7 ± 0.5	2.3 ± 0.3	11.5 ± 0.5	3.4 ± 0.2**	15.2 ± 0.6	3.2 ± 0.2**
4	Cell Count ($\times 10^6$ mL)	25 ± 0.5	5 ± 0.5	86 ± 0.5	10 ± 0.5	125 ± 0.5	12 ± 0.3**

Values are indicated in mean ± SEM, n = 6, one way ANOVA followed by Tukey's multiple comparison test. Statistical significant values were expressed as *$p < 0.05$ and **$p < 0.01$.

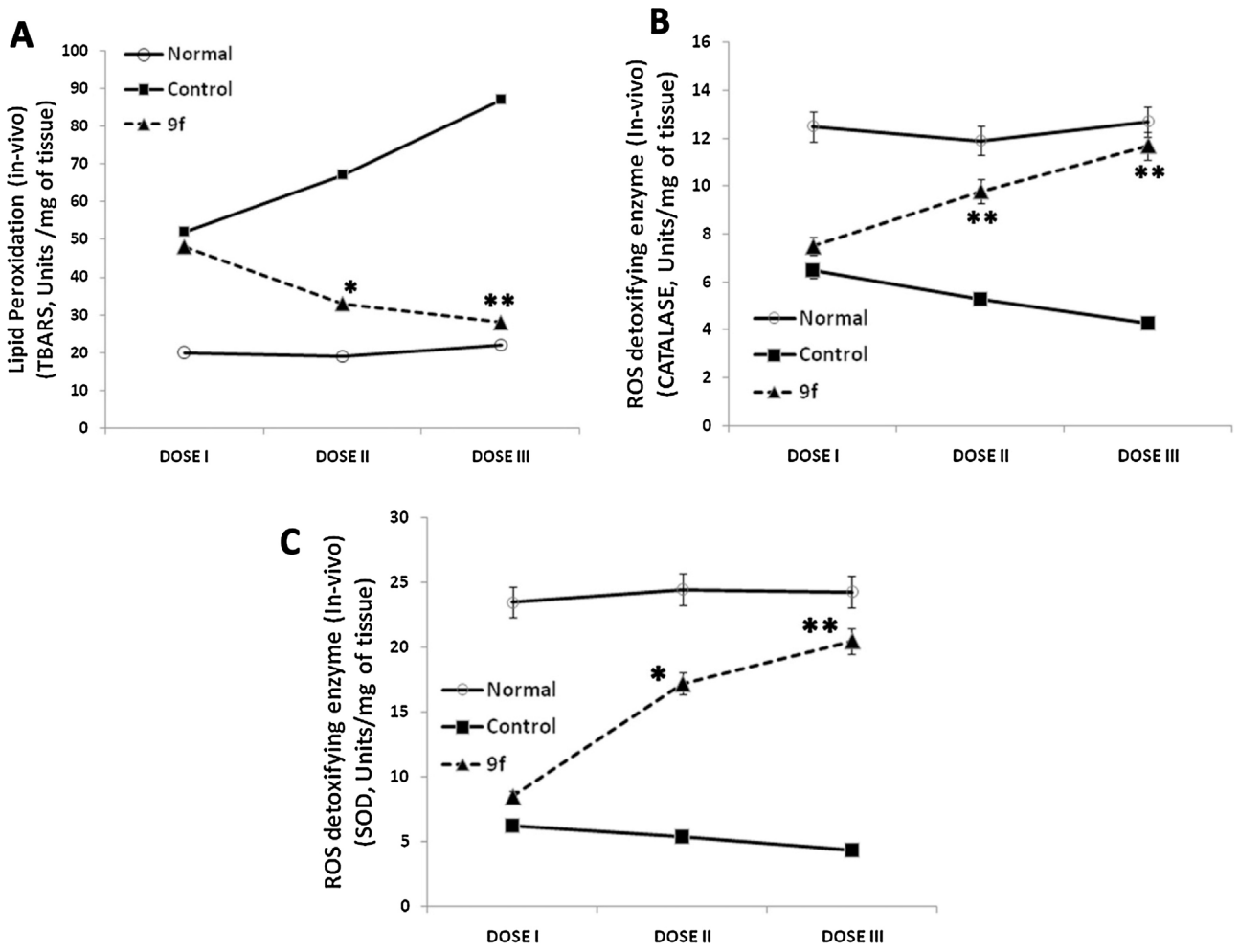

Fig. 2. Compound 9f potentially decelerates tumor induced lipid peroxidation and increases enzymic antioxidants. The elevated levels of lipid peroxidation and its breakdown product MDA is highly linked in tumorigenesis and neovasculature. The effect of compound **9f** in inhibiting the lipid peroxidation was determined by estimating MDA using TBARS assay. (A) Compound **9f** potently decreases the lipid peroxidation in dose dependant manner. Malignancy is associated with significantly altered ROS scavenging enzymes. Treatment with **9f** potentially elevates the hepatic catalase (B) and superoxide dismutase (C) in murine system. Results are the means of three independent determinations, conducted in triplicate. Statistically significant values are represented as*$p < 0.05$; **$p < 0.01$.

angiogenic complications and enlargement of peritoneal microvessels [34]. Our results inferred that compound **9f** significantly inhibited the peritoneal microvessels *in-vivo* as observed visibly in dose dependent manner (Fig. 3A). The angioinhibitory activity of compound **9f** was further validated by H & E stained peritoneal sections. Results showed that compound **9f** displayed a drastic reduction in microvessel density (MVD) in contrast to untreated animal confirming its angioinhibitory activity (Fig. 3B & C). Compelling evidences indicate that ROS promotes angiogenic signalling cascade governed by cytokines and transcription factors influencing tumor neovascularization [35,29]. ROS such as Superoxide anion ($O^{2}\cdot -$) and Hydrogen peroxide (H_2O_2) promote angiogenesis by inducing proangiogenic factors VEGF expression. Compound 9f detoxified ROS *in-vivo* by up regulating $O^{2}\cdot$ and H_2O_2scavengers such as SOD and catalase respectively in **9f** treated mice, as published reports have corroborated that over expression of those enzymes inhibited tumor neovascularization in mice [29]. Moreover by taking *in-vitro* ROS scavenging potential of compound **9f** into account (Fig. 1A), it is very evident that the compound attenuated angiogenesis most possibly through detoxifying the ROS radicals *in-vivo*. As indicated above, it has been postulated that main mechanism of oxidative stress induced angiogenesis involves peroxidized lipids and vascular endothelial growth factor (VEGF) signalling [3,35]. *In-vivo* observation infer that compound **9f** has potently decreased the VEGF levels in tumor bearing mice compared to that of control (Fig. 3D). Also, there was drastic reduction in the lipid peroxidation in **9f** treated animals as assessed by measuring thiobarbituric acid reactive substances (TBARS) *in-vivo* (Fig. 2A).The reduction of lipid peroxidation and peritoneal MVD with upregulated antioxidant enzymes has considerably influenced the survivability of **9f** treated animals (Fig. 3E). Henceforth these experimental observations provide a clear perspective that compound **9f** inhibits vascularization by quenching ROS and inducing antioxidant enzymes SOD and catalase, thereby leading to regressed VEGF levels and tumor cell proliferation.

3. Conclusion

The present study elucidated the synthesis of azo-hydrazone analogues as potent antioxidant molecules targeting disrupted ROS homeostasis in malignant and vascular progression. Among the synthetic series **9a–j**, compound **9f** emerged as the lead molecule with potent ROS scavenging and lipid peroxidation inhibitory activity. Compound **9f** significantly regressed the proliferation of Dalton's lymphoma ascites tumor cells and tumor angiogenesis by inhibiting VEGF levels *in-vivo*. Tumor growth index was paralleled with decreased ROS and lipid peroxide levels *in-vivo* and increased ROS detoxifying enzymes. Taking together, this study provides clear insight that compound **9f** by altering redox signalling components potently inhibited the tumor growth and tumor neovasculature. Hence azo-hydrazone

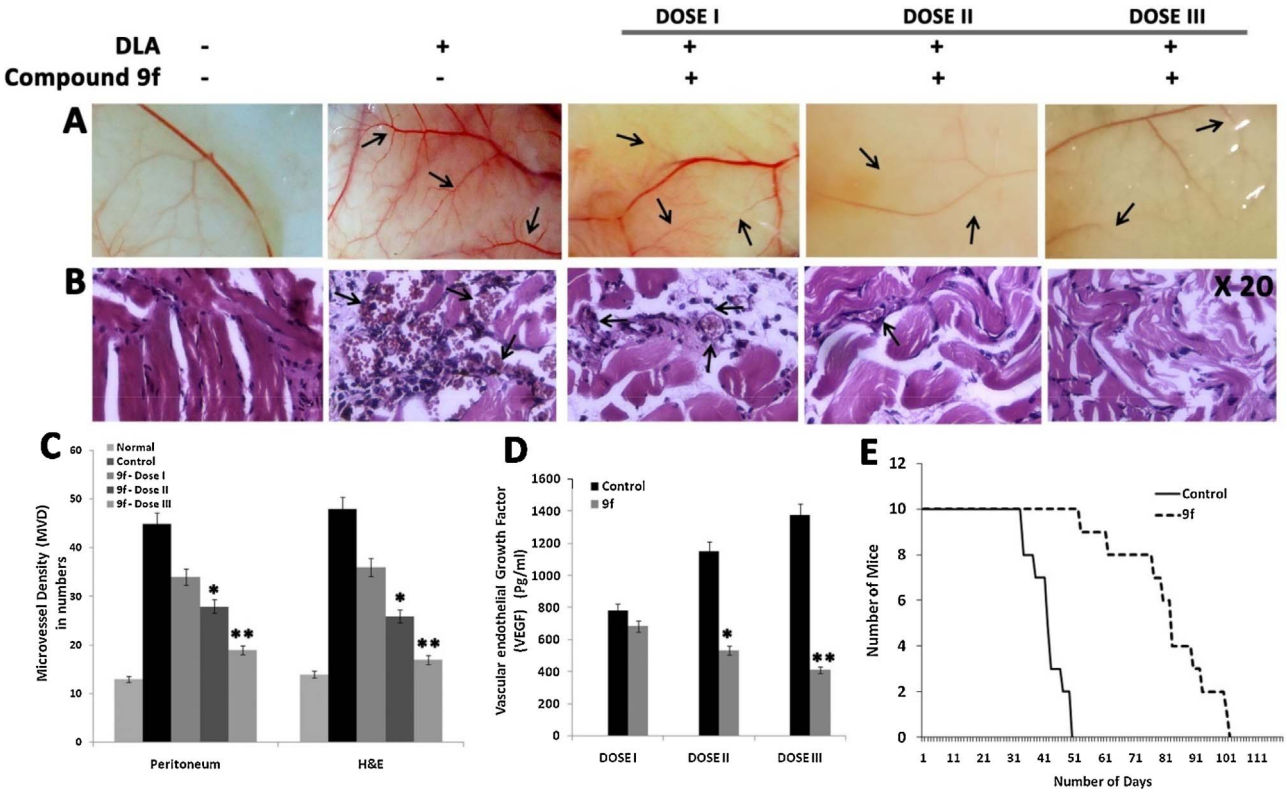

Fig. 3. Compound 9f regresses tumor neovascularization and vascular endothelial growth factor secretion in mice. To validate the angiopreventive effect of compound **9f**, DLA induced peritoneal angiogenesis was induced in mice by culturing DLA cells and administered with compound **9f** at 20 mg/kg *b.w.* (*i.p.*) for three consecutive doses on alternative day. (A) Compound **9f** antagonized the tumor induced peritoneal angiogenesis in dose dependant manner. (B) The angiogenesis inhibition was revalidated by H & E staining of the peritoneum. (C) The chart depicting the reduction of micro vascular density (MVD/HPF) in the peritoneum and H & E stained sections. (D) Compound **9f** inhibits VEGF-A secretion in tumor mice in dose dependant manner. (E) Kaplan–Meier graph showing the prolonged life span of **9f** treated mice.Statistically significant values are represented as*$p < 0.05$; **$p < 0.01$.

analogue **9f** could be developed as potential therapeutic molecule for malignant neoplasia and tumor angiogenesis targeting oxidant stress.

4. Materials and methods

4.1. Experimental section

All solvents and reagents, 2-hydroxypyridine, 8-hydroxyquinoline, 2-methyl-8-quinolinol, ethyl chloro acetate, hydrazine hydrate, benzaldehyde, o-tolualdehyde, 2-hydroxy-4-methoxybenzaldehyde, 5-chloro-2-nitrobenzaldehyde, aniline, 2-fluoroaniline, 2-bromoaniline, 2-chloroaniline, *p*-anisidine, commercial nano silica gel and $BF_3{\cdot}Et_2O$, DPPH, TBARS, TBA and MDA were purchased from Sigma Aldrich Chemicals Pvt Ltd. with a purity 90–99%. H_2O_2 was purchased from Merck Millipore, Massachusetts, United States. NBT and all other chemicals required for the experimental analysis were obtained from the Himedia, Mumbai, India. Recombinant VEGF was produced in Molecular Oncomedicine Laboratory, Sahyadri Science College, Shivamogga, Karnataka, India. TLC was performed on aluminum-backed silica plates and visualized by UV-light. Melting points (M.P) were determined on an electrically heated VMP-III melting point apparatus. The elemental analysis of the compounds was performed on a Perkin Elmer 2400 elemental analyzer. The results of elemental analyses were within ± 0.4% of the theoretical values. The FT-IR spectra were recorded using KBr discs and Nujol on FT-IR Jasco 4100 infrared spectrophotometer. ^{1}H NMR spectra were recorded on a Bruker 400 MHz NMR spectrometer in $CDCl_3$ or DMSO and the chemical shifts were recorded in parts per million downfield from tetramethylsilane. Mass spectra were recorded on LC–MS (API-4000) mass spectrometer.

4.2. Chemistry

4.2.1. General procedure for the synthesis of heteraryloxy-acetic acid ethyl ester *3a-c*

A mixture of heteroaryl hydroxy compounds **(1a–c**, 0.025 mol) and ethyl cholro acetate (**2**, 0.037 mol) in dry acetone (40 mL) with anhydrous potassium carbonate (0.037 mol) was refluxed for 10 h. The reaction mixture was cooled and the solvent was removed by distillation. The residual mass was triturated with cold water to remove potassium carbonate and extracted with ether (3 × 30 mL). The ether layer was washed with 10% sodium hydroxide solution (3 × 30 mL) followed by water (3 × 30 mL) and then dried over anhydrous sodium sulphate and *4.2.1.1. (Pyridin-2-yloxy)-acetic acid ethyl ester **3a***. Yield: 90%. M.P.: 158−160°C; IR (KBr) ν_{max} (cm^{-1}): 1680 (C═O), 1150 (C−O), 2900–3100 (C−H). ^{1}H NMR (400 MHz) ($CDCl_3$) δ (ppm): 1.43 (s, 3H, $CH_3$of ester), 4.32 (d, 2H, $CH_2$of ester), 4.91 (s, 2H, OCH_2), 6.5–7.6 (m, 4H, Ar-H).LC–MS *m/z* 182 (M + 1). Anal. Cal. for $C_9H_{11}NO_3$ (181): C, 59.66; H, 6.12; N, 7.73. Found: C, 59.62; H, 6.07; N, 7.69%.

4.2.2. (Quinolin-8-yloxy)-acetic acid ethyl ester 3b

Yield: 79%. M.P.: 116–118 °C; IR (KBr) ν_{max} (cm^{-1}): 1660 (C═O), 1130 (C−O), 2800–3000 (C−H). ^{1}H NMR (400 MHz) ($CDCl_3$) δ (ppm): 1.35 (t, 3H, $CH_3$of ester), 4.25 (d, 2H, $CH_2$of ester), 4.83 (s, 2H, OCH_2), 6.9–8.4 (m, 6H, Ar-H).LC–MS *m/z* 232 (M + 1). Anal. Cal. for $C_{13}H_{13}NO_3$ (231): C, 67.52; H, 5.67; N, 6.06. Found: C, 67.48; H, 5.63; N, 6.01%.

4.2.3. (2-Methyl-quinolin-8-yloxy)-acetic acid ethyl ester 3c

Yield: 84%. M.P.: 120–122 °C; IR (KBr) ν_{max} (cm^{-1}): 1635 (C═O), 1100 (C−O), 2850–3000 (C−H). ^{1}H NMR (400 MHz) ($CDCl_3$) δ (ppm): 1.39 (t, 3H, $CH_3$of ester), 2.32 (s, 3H, Ar-CH_3), 4.25 (s, 2H, $CH_2$of ester),

4.93 (s, 2H, OCH_2), 7.0–8.4 (m, 5H, Ar-H).LC–MS *m/z* 246 (M + 1). Anal. Cal. for $C_{14}H_{15}NO_3$ (245): C, 68.56; H, 6.16; N, 5.71. Found: C, 68.52; H, 6.11; N, 5.64%.

*4.2.4. General procedure for the synthesis of heteroaryl hydrazide **4a–c***

To compounds (**3a–c**, 0.01 mol) in ethanol (10 mL), 90% hydrazine hydrate (0.01 mol) was added in drops and stirred for 3 h at room temperature. A white solid was obtained. It wasfiltered and washed with water which on recrystalization with methanol afforded compounds **4a–c.**

*4.2.4.1. (Pyridin-2-yloxy)-acetic acid hydrazide **4a***. Yield: 76%. M.P.: 170–172 °C; IR (KBr) ν_{max} (cm^{-1}): 1645 (amide, C═O), 3205 (-NH-), $-NH_2$ show two bands one at 3200–3350 (-NH sym), 3300–3450 (−NH anti). ^{1}H MR (400 MHz) ($CDCl_3$) δ (ppm): 4.21 (s, 2H, NH_2), 4.83 (s, 2H, OCH_2), 6.5-7.7 (m, 4H, Ar-H), 9.5 (s, 1H, NH),.LC–MS *m/z* 168 (M + 1). Anal. Cal. for $C_7H_9N_3O_2$ (167): C, 50.29; H, 5.43; N, 25.14. Found: C, 50.25; H, 5.39; N, 25.08%.

4.2.4.2. (Quinolin-8-yloxy)-acetic acid hydrazide 4b. Yield: 80%. M.P.: 163–165 °C; IR (KBr) ν_{max} (cm^{-1}): 1655 (amide, C═O), 3200 (−NH−), $-NH_2$ show two bands one at 3230–3350 (−NH sym) and 3300–3450 (−NH anti). ^{1}H NMR (400 MHz) ($CDCl_3$) δ (ppm): 4.32 (s, 2H, NH_2), 4.84 (s, 2H, OCH_2), 7.1-8.7 (m, 6H, Ar-H), 9.3 (s, 1H, NH). LC–MS *m/z* 218 (M + 1). Anal. Cal. for $C_{11}H_{11}N_3O_2$ (217): C, 60.82; H, 5.10; N, 19.34. Found: C, 60.78; H, 5.06; N, 19.31%.

4.2.4.3. (2-Methyl-quinolin-8-yloxy)-acetic acid hydrazide 4c. Yield: 75%. M.P.: 159–161°C; IR (KBr) ν_{max} (cm^{-1}): 1643 (amide, C═O), 3180 (−NH−), $-NH_2$ show two bands one at 3200–3320 (−NH sym) and 3290–3350 (–NH anti). ^{1}H NMR (400 MHz) ($CDCl_3$) δ (ppm): 2.42 (s, 2H, CH_3), 4.43 (s, 2H, NH_2), 4.87 (s, 2H, OCH_2), 6.9–8.5 (m, 5H, Ar-H), 9.7 (s, 1H, NH). LC–MS *m/z* 232 (M + 1). Anal. Cal. for $C_{12}H_{31}N_3O_2$ (231): C, 62.33; H, 5.67; N, 18.17. Found: C, 62.29; H, 5.63; N, 18.12%.

4.2.5. Drying of ethanol (Super dry ethanol)

Ethyl alcohol of a high degree of purity is frequently required in preparative organic analysis. Ethyl alcohol was dry using quick lime (lumps of clean marble) was heated for 3–6 h in an oven at 200 °C. Rectified sprit (ethyl alcohol) was poured into R.B flasks containing freshly burned quick lime and the flask fitted with a doubled surface condenser carrying a dry $CaCl_2$ guard tube on top. The mixture was gently refluxed on an oil bath for six hours and allowed to stand overnight. It was then distilled it to have absolute ethyl alcohol. Super dry alcohol can be prepared from the product of dehydration of rectified sprit using activated magnesium. A clean dry magnesium (5 g) turnings and iodine (0.5 g) were placed in flask fallowed by 50–70 mL alcohol. The mixture was warmed until the iodine has disappeared, heating was continued until all the magnesium was converted into ethylate. Then, the absolute alcohol was added and the mixture was refluxed for 30 min, then alcohol was distilled off directly into the vessel in which it was stored. The reactions involved during the process are

$$CaCO_3 + H_2O \rightarrow Ca(OH)_2 + CO_2$$

$$Mg + 2C_2H_5OH \rightarrow H_2 + Mg(OC_2H_5)$$

$$Mg(OC_2H_5) + H_2O \rightarrow Mg(OH)_2 + 2C_2H_5OH$$

*4.2.6. General procedure for the synthesis of benzylidene hydrazones analogous **6a-g***

A mixture substituted aromatic aldehyde (**5a-d**, 0.01 mol) and heteroaryl hydrazide (**4a-c**, 1.37 g, 0.01 mol) in 15 mL of super dry ethanol was refluxed for 7 h with few drops of acid. The completion of reaction was confirmed by TLC. The reaction mixture was then poured into ice cold water and the precipitate obtained was filtered and dried in oven at low temperature. The product was recrystallised from absolute ethanol to afford compounds **6a–g** in a good yield.

4.2.6.1. (Pyridin-2-yloxy)-acetic acid (2-methyl-benzylidene)-hydrazone 6a. Yield: 90%. M.P.: 138–140 °C; IR (KBr) ν_{max} (cm^{-1}): 2930 (N−H), 1720 (C═O), 1499 (C═N), 1460 (C═C), 3120–3220 (amide, CO−NH). ^{1}H NMR (400 MHz) ($CDCl_3$) δ (ppm): 2.35 (s, 3H, CH_3), 4.72 (s, 2H, OCH_2), 6.5–7.8 (m, 8H, Ar-H), 8 0.5 (s, 1H, CH═N), 9.7 (s, 1H, NH). LC–MS *m/z* 270 (M + 1). Anal. Cal. for $C_{15}H_{15}N_3O_2$ (269): C, 66.90; H, 5.61; N, 15.60. Found: C, 66.86; H, 5.75; N, 15.57%.

4.2.6.2. (Pyridin-2-yloxy)-acetic acid (2-hydroxy-4-methoxy-benzylidene) -hydrazone 6b. Yield: 84%. M.P.: 116–118 °C; IR (KBr) ν_{max} (cm^{-1}): 2926 (N−H), 1715 (C═O), 1599 (C═N), 1472 (C═C), 3130–3230 (amide, CO−NH). ^{1}H NMR (400 MHz) ($CDCl_3$) δ (ppm): 3.53 (s, 3H, OCH_3), 4.8 (s, 2H, OCH_2), 6.2-7.7 (m, 7H, Ar-H), 8.7 (s, 1H, CH═N), 9.5 (s, 1H, NH), 10.3 (s, 1H, OH). LC–MS *m/z* 302 (M + 1). Anal. Cal. for $C_{15}H_{15}N_3O_4$ (301): C, 59.79; H, 5.02; N, 13.95. Found: C, 59.72; H, 4.95; N, 13.89%.

*4.2.6.3. (2-Methyl-quinolin-5-yloxy)-acetic acid (2-methyl-benzylidene)-hydrazone **6c***. Yield: 90%. M.P.: 112–114 °C; IR (KBr) ν_{max} (cm^{-1}): 2874 (N−H), 1690 (C═O), 1489 (C═N), 1535 (C═C), 3120–3220 (amide, CO−NH). ^{1}H NMR (400 MHz) ($CDCl_3$) δ (ppm): 2.33 (s, 3H, CH_3), 2.51 (s, 3H, CH_3), 4.67 (s, 2H, OCH_2), 7.4–8.1 (m, 9H, Ar-H), 8 0.6 (s, 1H, CH═N), 9.7 (s, 1H, NH). LC–MS *m/z* 334 (M + 1). Anal. Cal. for $C_{20}H_{19}N_3O_2$ (333): C, 72.05; H, 5.74; N, 12.60. Found: C, 71.95; H, 5.68; N, 12.57%.

*4.2.6.4. (Quinolin-8-yloxy)-acetic acid (2-methyl-benzylidene)-hydrazone **6d***. Yield: 92%. M.P.: 125–127 °C; IR (KBr) ν_{max} (cm^{-1}): 2956 (N−H), 1730 (C═O), 1553 (C═N), 1465(C═C), 3220–3310 (amide, CO−NH). ^{1}H NMR (400 MHz) ($CDCl_3$) δ (ppm): 2.39 (s, 3H, CH_3), 4.68 (s, 2H, OCH_2), 6.7–8.2 (m, 10H, Ar-H), 8.4 (s, 1H, CH═N), 9.9 (s, 1H, NH). LC–MS *m/z* 320 (M + 1). Anal. Cal. for $C_{15}H_{15}N_3O_2$ (319): C, 71.46; H, 5.37; N, 13.16. Found: C, 71.42; H, 5.31; N, 13.09%.

*4.2.6.5. (2-Methyl-quinolin-8-yloxy)-acetic acid (5-chloro-2-nitro-benzylidene)-hydrazone **6e***. Yield: 85%. M.P.: 137–139 °C; IR (KBr) ν_{max} (cm^{-1}): 2945 (N−H), 1740 (C═O), 1523 (C═N), 1520 (C═C), 3130–3230 (amide, CO−NH). ^{1}H NMR (400 MHz) ($CDCl_3$) δ (ppm): 2.35 (s, 3H, CH_3), 4.80 (s, 2H, OCH_2), 6.5–7.8 (m, 8H, Ar-H), 8 0.5 (s, 1H, CH═N), 9.7 (s, 1H, NH). LC–MS *m/z* 399 (M + 1). Anal. Cal. for $C_{19}H_{15}ClN_4O_4$ (398): C, 57.22; H, 3.79; N, 14.05. Found: C, 57.17; H, 3.73; N, 13.96%.

*4.2.6.6. (2-Methyl-quinolin-8-yloxy)-acetic acid (2-hydroxy-4-methoxy-benzylidene)-hydrazone **6f***. Yield: 87%. M.P.: 110–113 °C; IR (KBr) ν_{max} (cm^{-1}): 2935 (N−H), 1690 (C═O), 1512 (C═N), 1454 (C═C), 3100–3215 (amide, CO−NH). ^{1}H NMR (400 MHz) ($CDCl_3$) δ (ppm): 2.36 (s, 3H, CH_3), 3.52 (s, 3H, OCH_3), 4.69 (s, 2H, OCH_2), 6.3–8.2 (m, 8H, Ar-H), 8.1 (s, 1H, CH═N), 10.2 (s, 1H, NH), 10.5 (s, 1H, OH). LC–MS *m/z* 366 (M + 1). Anal. Cal. for $C_{20}H_{19}N_3O_4$ (365): C, 65.74; H, 5.24; N, 11.50. Found: C, 65.71; H, 5.19; N, 11.44%.

*4.2.6.7. (Quinolin-8-yloxy)-acetic acid benzylidene-hydrazone **6g***. Yield: 78%. M.P.: 135–137 °C; IR (KBr) ν_{max} (cm^{-1}): 2894 (N−H), 1715 (C═O), 1567 (C═N), 1493 (C═C), 3110–3210 (amide, CO−NH). ^{1}H NMR (400 MHz) ($CDCl_3$) δ (ppm): 4.73 (s, 2H, OCH_2), 7.1-8.3 (m, 11H, Ar-H), 8 0.6 (s, 1H, CH═N), 10.5 (s, 1H, NH). LC–MS *m/z* 306 (M + 1). Anal. Cal. for $C_{18}H_{15}N_3O_2$ (305): C, 70.81; H, 4.95; N, 13.76. Found: C, 70.78; H, 4.89; N, 13.71%.

4.2.7. Preparation of 15 mol% nano $BF_3{\cdot}SiO_2$

Nano $BF_3{\cdot}SiO_2$ was easily prepared from nano silica gel and $BF_3{\cdot}Et_2O$

according to the literature. In short, $BF_3{\cdot}Et_2O$ (2.65 mL) was added drop-wise to a slurry containing nano silica gel (7 g) and ethanol (30 mL, instead of chloroform). The mixture was stirred for 1 h at room temperature. The resulted suspension was filtered to obtain the white solid named nano $BF_3{\cdot}SiO_2$ (15 mol%). The acidic capacity of nano $BF_3{\cdot}SiO_2$ was 2.07 $mmolg^{-1}$ and determined via titration of 0.2 g of solid acid with standard solution of NaOH [36].

4.2.8. General procedure for the synthesis of (hetero-aryloxy)-acetic acid (phenylazo-methylene)-hydrazone (Azo-hydrazone analogues)

Benzylidine hydrazone analogous **6a–g** were dissolved in ethanolic solution of sodium hydroxide (15 mL). The mixture was cooled down to 0 °C and kept ready for the coupling reaction (stock solution). At the other side, substituted aryl diazonium salt **8a–e** were prepared with subsituted aniline **7a–e** by diazotization using nano $BF_3{\cdot}SiO_2$ as a catalyst.

diazotization (To synthesize aryldiazonium salts **8a–e**, aromatic amines **7a–e** (4 mmol) was stirred with $NaNO_2$ (5 mmol) using nano $BF_3{\cdot}SiO_2$ as a catalyst at −5–0 °C). This diazonium solution was added in drop wise manner to basic buffer solutions as prepared above. The residual acidic sites on nano $BF_3{\cdot}SiO_2$ in diazotization step can partially decompose benzylidine hydrazone analogous to the starting materials in non-basic medium. So, NaOH amount should be sufficient before adding of aryl diazonium salts (Medium pH of 10–12 is suitable). Reaction mixture cooled down to 0 °C, in ice bath with constant stirring for the coupling reaction. Care was taken for to not let temperature exceed −5–0 °C. The mixture was stirred for 3–4 h at the same temperature. After completion of the reaction (TLC), the mixture was washed with distilled water (50 mL) for naturalization of additional NaOH and then by acetone (30 mL) for separation of nano $BF_3{\cdot}SiO_2$. Evaporation of the solvent followed by column chromatography afforded compounds **9a–j** in good yields. The compound was recrystallized from methanol to obtained pure product **9a–j.**

*4.2.8.1. (Pyridin-2-yloxy)-acetic acid (phenylazo-o-tolyl-methylene)-hydrazone **9a***. Yield: 90%. M.P.: 114–116 °C; IR (KBr) ν_{max} (cm^{-1}): 2930 (N−H), 1563 (C=N), 1459 (C=C), 1454 (N=N), 3120–3220 (amide, CO−NH). ^{1}H NMR (400 MHz) ($CDCl_3$) δ (ppm): 2.28 (s, 3H, CH_3), 4.68 (s, 2H, OCH_2), 6.6-7.8 (m, 13H, Ar-H), 9.8 (s, 1H, NH). ^{13}C NMR (DMSO-d_6) δ: 175.8, 166.2, 160.7, 149.5, 140.2, 138.4, 137.5, 135.7, 133.8, 131.3, 128.4, 125.3 120.6, 109.3, 80.1, 16.2. LC–MS *m/z* 374.17 (M + 1). Anal. Cal. for $C_{21}H_{19}N_5O_2$ (373.15): C, 67.55; H, 5.13; N, 18.76. Found: C, 67.55; H, 5.13; N, 18.76%.

*4.2.8.2. (Pyridin-2-yloxy)-acetic acid [(4-methoxy-phenylazo)-o-tolyl-methylene]-hydrazone **9b***. Yield: 85%. M.P.: 110–112 °C; IR (KBr) ν_{max} (cm^{-1}): 2920 (N−H), 1480 (C=N), 1531 (C=C), 1460 (N=N), 3120–3220 (amide, CO−NH). ^{1}H NMR (400 MHz) ($CDCl_3$) δ (ppm): 2.26 (s, 3H, CH_3), 3.8 (s, 3H, OCH_3), 4.68 (s, 2H, OCH_2), 6.8–7.7 (m, 12H, Ar-H), 9.7 (s, 1H, NH). ^{13}C NMR (DMSO-d_6) δ: 174.3, 165.1, 161.7, 154.6, 148.5, 140.2, 139.7, 138.4, 133.8, 130.5, 128.3, 127.6, 125.3, 120.6, 119.8, 117.1, 111.8, 80.8, 57.5, 17.6. LC–MS *m/z* 404.18 (M + 1). Anal. Cal. for $C_{22}H_{21}N_5O_3$ (403.16): C, 65.50; H, 5.25; N, 17.36. Found: C, 65.43; H, 5.21; N, 17.29%.

*4.2.8.3. (Pyridin-2-yloxy)-acetic acid [(2-fluoro-phenylazo)-(2-hydroxy-4-methoxy-phenyl)-methylene]-hydrazone **9c***. Yield: 88%. M.P.: 121–123 °C; IR (KBr) ν_{max} (cm^{-1}): 2915 (N−H), 1489 (C=N), 1568 (C=C), 1115 (C-F), 1475 (N=N), 3110–3210 (amide, CO−NH). ^{1}H NMR (400 MHz) ($CDCl_3$) δ (ppm): 3.7 (s, 3H, OCH_3), 4.72 (s, 2H, OCH_2), 6.5–7.7 (m, 11H, Ar-H), 9.5 (s, 1H, NH), 10.3 (s, 1H, OH). ^{13}C NMR (DMSO-d_6) δ: 173.8, 168.73, 166.1, 162.8, 158.7, 156.3, 148.6, 139.3, 130.4, 130.8, 123.7, 117.1, 115.6, 109.7, 108.5, 104.8, 99.6, 83.2, 53.4. LC–MS *m/z* 424.13 (M + 1). Anal. Cal. for $C_{21}H1_8FN_5O_4$ (423.13): C, 59.57; H, 4.29; N, 16.54. Found: C, 59.49; H, 4.25; N, 16.51%.

*4.2.8.4. (2-Methyl-quinolin-8-yloxy)-acetic acid [(2-bromo-phenylazo)-o-tolyl-methylene]-hydrazone **9d***. Yield: 78%. M.P.: 118–120 °C; IR (KBr) ν_{max} (cm^{-1}): 2930 (N−H), 1499 (C=N), 1530 (C=C), 568 (C-Br), 1460 (N=N), 3120–3220 (amide, CO−NH). ^{1}H NMR (400 MHz) ($CDCl_3$) δ (ppm): 2.24 (s, 3H, CH_3), 2.29 (s, 3H, CH_3), 4.81 (s, 2H, OCH_2), 6.7-8.5 (m, 13H, Ar-H), 9.7 (s, 1H, NH). ^{13}C NMR (DMSO-d_6) δ: 174.2, 159.5, 155.9, 155.3, 139.9, 138.2, 134.2, 132.9, 132.5, 131.5, 130.7, 129.3, 128.9, 128, 127.8 126.6, 125.3, 123.4, 123, 119.1, 106.3, 78.3, 21.3, 16.2. LC–MS *m/z* 516.15 (M + 1). Anal. Cal. for $C_{26}H_{22}BrN_5O_2$ (515.10): C, 60.47; H, 4.29; N, 13.56. Found: C, 60.43; H, 4.22; N, 13.53%.

*4.2.8.5. (Quinolin-8-yloxy)-acetic acid (phenylazo-o-tolyl-methylene)-hydrazone **9e***. Yield: 75%. M.P.: 135–37 °C; IR (KBr) ν_{max} (cm^{-1}): 2956 (N−H), 1512 (C=N), 1496 (C=C), 1453 (N=N), 3140–3250 (amide, CO−NH). ^{1}H NMR (400 MHz) ($CDCl_3$) δ (ppm): 2.27 (s, 3H, CH_3), 4.68 (s, 2H, OCH_2), 6.9–8.8 (m, 15H, Ar-H), 9.6 (s, 1H, NH). ^{13}C NMR (DMSO-d_6) δ: 175.6, 159.6, 157.5, 148.2, 139.8, 137.2, 135.8, 130.9, 129.7, 127.3, 126.8, 126.1, 125.4, 123.8, 122.6, 120.1, 118.7, 105.3, 80.4, 15.3. LC–MS *m/z* 424.20 (M + 1). Anal. Cal. for $C_{25}H_{21}N_5O_2$ (423.17): C, 70.91; H, 5.00; N, 16.54. Found: C, 70.85; H, 4.96; N, 16.48%.

*4.2.8.6. (2-Methyl-quinolin-8-yloxy)-acetic acid [(5-chloro-2-nitro-phenyl)-(2-chloro-phenylazo)-methylene]-hydrazone **9f***. Yield: 68%. M.P.: 146–148 °C; IR (KBr) ν_{max} (cm^{-1}): 2930 (N−H), 1595 (C=N), 1543 (C=C), 724 (C−Cl), 1354 (NO_2), 1470 (N=N), 3120–3220 (amide, CO−NH). ^{1}H NMR (400 MHz) ($CDCl_3$) δ (ppm): 2.27 (s, 3H, CH_3), 4.71 (s, 2H, OCH_2), 6.7–8.4 (m, 12H, Ar-H), 9.7 (s, 1H, NH). ^{13}C NMR (DMSO-d_6) δ: 174.6, 160.3, 157.9, 156.2, 149.0, 143.3, 140.8, 137.1, 135.3, 133.7, 131.3, 130, 129.5, 128.7, 127.8, 127, 125.1, 125.3, 122.1, 119.2, 108.7, 76.4, 19.3. LC–MS *m/z* 537.11 (M + 1). Anal. Cal. for $C_{25}H_{18}Cl_2N_6O_4$ (536.08): C, 55.88; H, 3.38; N, 15.64. Found: C, 55.82; H, 3.33; N, 15.58%.

*4.2.8.7. (2-Methyl-quinolin-8-yloxy)-acetic acid [(2-hydroxy-4-methoxy-phenyl)-(4-methoxy-phenylazo)-methylene]-hydrazone **9g***. Yield: 90%. M.P.: 128–130 °C; IR (KBr) ν_{max} (cm^{-1}): 2960 (N−H), 1512 (C=N), 1613 (C=C), 1476 (N=N), 3220–3320 (amide, CO−NH). ^{1}H NMR (400 MHz) ($CDCl_3$) δ (ppm): 2.26 (s, 3H, CH_3), 3.8 (s, 6H, OCH_3), 4.68 (s, 2H, OCH_2), 6.2-8.5 (m, 12H, Ar-H), 9.8 (s, 1H, NH), 10.3 (s, 1H, 0H). ^{13}C NMR (DMSO-d_6) δ: 175.2, 166.7, 163.2, 159.6, 158.8, 155.6, 154.4, 148.8, 133.4, 131.2, 130.0, 128.8, 122.9, 121.7, 119.7, 116.9, 113.8, 110.7, 107.8, 102.9, 101.4, 78.7, 56.0, 21.3. LC–MS *m/z* 500.23 (M + 1). Anal. Cal. for $C_{27}H_{25}N_5O_5$ (499.19): C, 64.92; H, 5.04; N, 14.0. Found: C, 64.88; H, 4.98; N, 13.96%.

*4.2.8.8. (Pyridin-2-yloxy)-acetic acid [(2-chloro-phenylazo)-(2-hydroxy-4-methoxy-phenyl)-methylene]-hydrazone **9h***. Yield: 75%. M.P.: 154–156 °C; IR (KBr) ν_{max} (cm^{-1}): 2924 (N−H), 1562 (C=N), 1512 (C=C), 673 (C−Cl), 1499 (N=N), 3120–3220 (amide, CO−NH). ^{1}H NMR (400 MHz) ($CDCl_3$) δ (ppm): 3.68 (s, 3H, OCH_3), 4.72 (s, 2H, OCH_2), 6.4–7.8 (m, 11H, Ar-H), 9.4 (s, 1H, NH). ^{13}C NMR (DMSO-d_6) δ: 173.9, 166.5, 164.1, 159.8, 155.3, 149.6, 138.8, 134.5, 131.4, 130.4, 128.7, 127.4, 115.1, 110.3, 109.7, 106.3, 102.4, 78.5, 53.9. LC–MS *m/z* 440.14 (M + 1). Anal. Cal. for $C_{21}H_{18}ClN_5O_4$ (439.10): C, 57.34; H, 4.12; N, 15.92. Found: C, 57.31; H, 4.06; N, 15.89%.

*4.2.8.9. (Pyridin-2-yloxy)-acetic acid [(2-bromo-phenylazo)-o-tolyl-methylene]-hydrazone **9i***. Yield: 90%. M.P.: 136–137 °C; IR (KBr) ν_{max} (cm^{-1}): 2930 (N−H), 1515 (C=N), 1457 (C=C), 551 (C-Br), 1456 (N=N), 3140–3230 (amide, CO−NH). ^{1}H NMR (400 MHz) ($CDCl_3$) δ (ppm): 2.32 (s, 3H, CH_3), 4.68 (s, 2H, OCH_2), 6.4–7.7 (m, 12H, Ar-H), 9.9 (s, 1H, NH). ^{13}C NMR (DMSO-d_6) δ: 176.5, 168.2, 159.8, 150.6, 141.3, 137.8, 135.9, 132.4, 131.8, 130.4, 129.2, 128.9, 127.5, 124.6, 122.5, 116.3, 115.5, 80.3, 15.5. LC–MS *m/z* 452.11 (M + 1). Anal. Cal.

for $C_{21}H_{18}BrN_5O_2$ (451.06): C, 55.76; H, 4.01; N, 15.48. Found: C, 55.72; H, 3.95; N, 15.41%.

4.2.8.10. (Quinolin-8-yloxy)-acetic acid [(2-methoxy-phenylazo)-phenyl-methylene]-hydrazone ***9j***. Yield: 89%. M.P.: 143–145 °C; IR (KBr) ν_{max} (cm^{-1}): 2945 (N—H), 1514 (C═N), 1620 (C═C),1480 (N═N), 3120–3220 (amide, CO—NH). ^{1}H NMR (400 MHz) ($CDCl_3$) δ (ppm): 3.81 (s, 3H, OCH_3), 4.67 (s, 2H, OCH_2), 7.1–8.6 (m, 15H, Ar-H), 9.6 (s, 1H, NH). ^{13}C NMR (DMSO-d_6) δ: 175.3, 165.8, 159.3, 155.8, 150.4, 142.0, 137.8, 135.3, 131.8, 130.3, 129.3, 128.8, 127.6, 126.1, 123.5, 122.1, 119.3, 114, 108.9, 78.5, 55.3. LC–MS *m/z* 440.17 (M + 1). Anal. Cal. for $C_{25}H_{21}N_5O_3$ (439.16): C, 68.33; H, 4.82; N, 15.94. Found: C, 68.29; H, 4.77; N, 15.90%.

4.3. Pharmacology

4.3.1. DPPH photometric assay

The DPPH radical scavenging activity of the synthesized azo-hydrazone analogues was evaluated as described earlier with slight modification [37]. Briefly, 2.5 mL of 0.2 mM DPPH methanol solution along with each compound (**9a–j** series) in different concentration range (1–200 μg/mL) was mixed well and incubated in dark at room temperature. After 30 min absorbance was read at 518 nm. Ascorbic acid was used as a positive control.

4.3.2. Hydrogen peroxide scavenging assay

The H_2O_2 radical scavenging activity of the azo-hydrazone analogues (**9a–j**) was determined as described previously [38]. Briefly, 2 mM of H_2O_2 solution was prepared in 50 mM phosphate buffer pH 7.4. The synthetic drugs **9a–j** series (0.1 mL of 1–200 μg/mL concentration) were mixed with 0.4 mL of 50 mM phosphate buffer (pH 7.4). Then, 0.6 mL H_2O_2 solution was added and the absorbance was read at 230 nm.

4.3.3. Superoxide scavenging assay

Compound **9a–j** series was subjected to scavenging activity for superoxide anion radical ($O_2^{\cdot -}$) generated by NADH/PMS system according to previous methods with slight modifications [39]. Shortly, the reaction mixture consisted of **9a–j** series (1–200 μg/mL concentration), 166 μM NADH, 107.5 μM NBT and 2.7 μM PMS dissolved in 19 mM of potassium phosphate buffer (pH 7.4). After 5 min of incubation at 25 °C, absorbance was measured at 560 nm using eppendorf spectrophotometer.

4.3.4. In-vitro lipid peroxidation assay

The effect of compound **9a–j** series on *in-vitro* lipid peroxidation was performed by the methods as described earlier by measuring thiobarbituric acid reactive substances (TBARS) with slight modifications [40]. Analyses were done using total mice liver homogenate in cold 50 mM phosphate buffer (plus KCl 125 mM). The reactions were started by addition of Fe(II) to solutions (0.5 mL final volume) containing 10 mM phosphate (pH 7.2), KCl 125 mM, 5% v/v liver homogenate, compound **9a–j** and H_2O_2. This was followed by the addition of 0.2 mL 7% phosphoric acid plus 0.2 mL TBA solution to the reaction mixture. After 15 min of boiling, solutions were cooled and absorbance was read at 532 nm.

4.4. Anti-tumor activity and angiogenesis studies

4.4.1. Animal and ethical statement

Swiss albino mice aged 5–6 weeks, weighing 25–30 g were housed under standard laboratory conditions and fed with commercial rodent meal and water ad libitum. All the animal experimentations were approved by the Institutional Animal Ethics Committee (IAEC), National College of Pharmacy, Shimoga, India, in accordance with the Committee for the Purpose of Control and Supervision of Experiments on Animals (CPCSEA) guidelines for laboratory animal facility (NCP/IAEC/CL/101/05/2012-13).

4.4.2. Animal tumor models and treatment

DLA cells were cultured *in-vivo* by intra-peritoneal *(i.p)* transplantation to develop ascites tumor by adopting previous reports [34]. After the optimal growth of the tumor, three doses of **9f** were administered to test mice at a concentration 20 mg/kg body weight through intraperitoneal route. On day 10 after the final treatment, ascitic lymphoma growth parameters including percentage of tumor inhibition, ascites secretion and tumor cell counts were analyzed. The number of animals survived and the life span duration after the treatment period were documented separately. To examine the physiological effect of **9f** in normal non-tumor mice, the serum of **9f** treated animals were subjected to the estimation of alkaline phosphatase (ALP), creatinine and urea. Liver and spleen were surgically removed from test and control animals for the histopathological analysis.

4.4.3. Peritoneal microvessel density (MVD) assessement

The angiogenic response of compound **9f** in tumor condition was assessed by peritoneal microvessel density and H & E staining as described previously [30]. Shortly, the formaldehyde-fixed peritoneum of the control and **9f**treated were processed for H & E staining. Then quantification of MVD was performed using light optical microscopy in the areas of peritoneum containing the highest number of capillaries.

4.4.4. In-vivo lipid peroxidation assay

In-vivo lipid peroxidation in the compound **9f** treated and control tumor bearing animals were done as per the previously described methods [41]. Briefly, the whole liver was dissected out and a 10% tissue homogenate was prepared in ice cold 100 mM PBS pH-7.2. Liver tissue homogenate of the control and **9f** treated were the estimation of lipid peroxidation.

4.4.5. Assays for in-vivo hepatic antioxidant enzyme

Hepatic antioxidant enzyme Superoxide dismutase and catalase were estimated in the **9f** treated and control tumor bearing animals as per the previous protocols [31]. Liver tissue homogenate of control and **9f** treated mice were used for the estimation of enzyme levels.

4.4.6. VEGF-ELISA

The *in-vivo* secretion of VEGF was quantified in serum of control and **9f** treated DLA bearing mice by ELISA as per described protocols [42,43]. On note, 100 μL of serum from the control and **9f** treated were coated in a coating buffer at 4 °C overnight. Subsequently, wells were incubated with anti-VEGF-A antibodies (Sigma Aldrich, USA), followed by re-incubation with secondary antibodies tagged to alkaline phosphatase. VEGF-A was measured by reading the absorbance at 405 nm using PNPP as substrate.

4.5. Statistical analysis

Values were expressed as mean ± standard error (SEM). Statistical significance was evaluated by one-way analysis of variance (ANOVA) followed by Student's *t*-test ($^*p < 0.05$) and ($^{**}p < 0.01$).

Acknowledgements

Zabiulla gratefully acknowledges the financial support provided by the Department of Science and Technology, New Delhi, Under INSPIRE-Fellowship scheme [IF140407]. Shaukath Ara Khanum thankfully acknowledges the financial support provided by VGST, Bangalore, under CISEE Programme [Project sanction order: No. VGST/CISEE/282]. B.T. Prabhakar gratefully acknowledges the grant extended by DBT (6242-P37/RGCB/PMD/DBT/PBKR/2015), UGC(F.No.41-507/2012 (SR) and VGST (VGST/GRD231/CISEE/2013-14).

Appendix A. Supplementary data

Supplementary data associated with this article can be found, in the online version, at http://dx.doi.org/10.1016/j.biopha.2017.08.076.

References

[1] E. Panieri, M.M. Santoro, ROS homeostasis and metabolism: a dangerous liason in cancer cells, Cell Death Dis. 7 (2016) 2253.
[2] Geou-Yarh Liou, Peter Storz, Reactive oxygen species in cancer, Free Radic. Res. 44 (5) (2010) 1–57.
[3] Young-Woong Kim, Tatiana V. Byzova, Oxidative stress in angiogenesis and vascular disease, Blood 123 (2014) 625–631.
[4] Paul T. Schumacker, Reactive oxygen species in cancer: a dance with the devil, Cancer Cell 27 (2015) 156–157.
[5] S.A. Khanum, S. Shashikanth, S. Umesha, R. Kavitha, Synthesis and antimicrobial study of novel heterocyclic compounds from hydroxyl benzophenones, Eur. J. Med. Chem. 40 (2005) 1156–1162.
[6] T. Prashanth, P. Thirusangu, B.R. Vijay Avin, V. Lakshmi Ranganatha, B.T. Prabhakar, S.A. Khanum, Synthesis and evaluation of novel benzophenone-thiazole derivatives as potent VEGF-A inhibitors, Eur. J. Med. Chem. 87 (2014) 274–283.
[7] Zabiulla, H.G. Shamanth Neralagundi, A. Bushra Begum, B.T. Prabhakar, S.A. Khanum, Design and synthesis of diamide-coupled benzophenones as potential anticancer agents, Eur. J. Med. Chem 115 (2016) 342–351.
[8] G. Turan-Zitouni, Y. Blache, K. Güven, Boll. Chim.Farm. 140 (2001) 397–400.
[9] P. Gao, Y. Wei, Efficient oxidative cyclization of *N*-acylhydrazones for the synthesis of 2, 5-disubstituted 1, 3, 4-oxadiazoles using *t*-BuOI under neutral conditions, Heterocycl. Commun. 19 (2) (2013) 113–119.
[10] J. Chang, G. Huang, H. Liu, W. Yu, Y. Zhang, J. Chang, L. Dong, Y. Li, Yu Xuejun, I_2 mediated oxidative C-O bond formation for the synthesis of 1, 3, 4-Oxadiazoles from aldehydes and hydrazides, J. Org. Chem. 78 (2013) 10337–103431.
[11] F. Lamaty, C. Martin, J. Martinez, P. Nun, Tetrahedron 67 (2013) 8187–8194.
[12] Ke Chen, Yang Hu, Qing-Shan Li, Xiang Lu, Ru Yan, Hai-Liang Zhu, Bioorg. Med. Chem. 20 (2012) 903–909.
[13] N. Jacobsen, Eric Tan, L. Kian, Angewandte Chemie − Int. Edition. 46 (2007) 1315–13171.
[14] Z.D. Liu, R.C. Hider, Coord. Chem. Rev. 232 (2002) 151.
[15] T.F. Tam, R. Leung-Toung, W.R. Li, Y.S.K. Wang, M. Karimian, Curr. Spino, Med. Chem. 10 (2003) 983.
[16] B.C. Bruna, N.M. Mauro, O. Thayse de, O. Luís Flavio de, M.M. Michel, M.F. Alexandre, G. Grace, C.B.G. Simone, Synthesis and biological evaluation of hydrazone derivatives as antifungal agents, Molecules 20 (5) (2015) 9229–9241.
[17] P. Melnyk, V. Leroux, C. Sergheraert, P. Grellier, Bioorg. Med. Chem. Lett. 16 (2006) 31.
[18] S. Rollas, S.G. Kucukguzel, Biological activities of hydrazone derivatives, Molecules 12 (2007) 1910–1939.
[19] R. Narang, B. Narasimhan, S. Sharma, Curr. Med. Chem. 19 (2012) 569.
[20] E. Mackova, K. Hruskova, P. Bendova, A. Vavrova, H. Jansova, P. Haskova, P. Kovarikova, K. Vavrova, T. Simunek, Methyl and ethyl ketone analogs of salicylaldehyde isonicotinoyl hydrazone: novel iron chelators with selective antiproliferative action, Chem. Biol. Interact. 197 (2012) 69.
[21] C.M. Mustapha, T., Bapu, S., Dnyaneshwar, Y., Ramesh, Synthesis and Biological Evaluation of New Hydrazone Derivatives of Quinoline and Their Cu(II) and Zn(II) Complexes against Mycobacterium tuberculosis, 2015, https://dx.doi.org/10.1155/2015/153015.
[22] H.G. Garg, R.A. Sharma, J. Med. Chem. 12 (1996) 1122.
[23] A.A. Jarahpour, M. Motamedifar, K. Pakshir, N. Hadi, Z. Zarei, Molecules 9 (2004) 815–824.
[24] S. Samadhiya, H. Halve, Synthetic utility of Schiff bases as potential herbicidal agents, Oriental J Chem 17 (2001) 119–122.
[25] K.M. Rathod, N.S. Thakre, Synthesis and antimicrobial activity of azo compounds containing *m*-Cresol moiety, Chem. Sci. Trans. 2 (1) (2013) 25–28.
[26] T.A. Farghaly, Z.A. Abdullah, Synthesis, azo-hydrazone tautomerism and antitumor screeningof N-(3-ethoxycarbonyl-4, 5, 6, 7-tetrahydro-benzo[b]thien-2-yl)-2 arylhydrazono ?3- oxobutanamide derivatives, ARKIVOC17 295 (2008).
[27] H. Xu, X. Zeng, Bioorg. Med. Chem. Lett. 20 (2010) 4193.
[28] Shahzad Murtaza, Jamshaid Ashraf, Asian J. Chem. 27 (10) (2015) 3551–3554.
[29] Masuko Ushio-Fukai, Yoshimasa Nakamura, Reactive oxygen species and angiogenesis: NADPH oxidase as target for cancer therapy, Cancer Lett. 266 (1) (2008) 37–52.
[30] M. Al-Ghorbani, V. Vigneshwaran, V.L. Ranganatha, B.T. Prabhakar, S.A. Khanum, Synthesis of oxadiazole?morpholine derivatives and manifestation of the repressed CD31 microvessel density (MVD) as tumoral angiogenic parameters in Dalton's Lymphoma, Bioorg. Chem. 60 (2015) 136–146.
[31] P. Thirusangu, V. Vigneshwaran, B.R. Vijay Avin, H. Rakesh, H.M. Vikas, B.T. Prabhakar, Scutellarein antagonizes the tumorigenesis by modulating cytokine VEGF mediated neoangiogenesis and DFF-40 actuated nucleosomal degradation, Biochem. Biophys. Res. Commun. 484 (2017) 85–92.
[32] Abigail Hielscher, Sharon Gerecht, Hypoxia and free radicals: role in tumor progression and the use of engineering-based platforms to address these relationships, Free Radic. Biol. Med. 79 (2015) 281–291.
[33] Gina Manda, Marina tamara nechifor, teodora-Monica neagu, reactive oxygen species, cancer and anti-cancer therapies, Curr.t Chem. Biol. 3 (2009) 342–366.
[34] V. Vigneshwaran, P. Thirusangu, S. Madhusudana, V. Krishna, S.N. Pramod, B.T. Prabhakar, The latex sap of the 'Old World Plant' Lagenaria siceraria with potent lectin activity mitigates neoplastic malignancy targeting neovasculature and cell death, Int. Immunopharmacol. 39 (2016) 158–171.
[35] S.C. Bir, G.K. Kolluru, K. Fang, C.G. Kevil, Redox balance dynamically regulates vascular growth and remodeling, Semin. Cell Dev. Biol. 23 (7) (2012) 745–757.
[36] B.F. Mirjalili, A. Bamoniri, A. Akbari, One-Pot synthesis of 3,4-Dihydropyrimidin-2(1H)-ones (Thiones) promoted by $NanoBF_3.SiO_2$, J. Iran. Chem. Soc. 8 (2011) 135–140.
[37] B.C. Goudarshivanavar, V. Vigneshwaran, K.K. Dharmappa, S.N. Pramod, Pharmacological potential of Tetrahydrofurano/Pyrano quinoline and benzo[b] furoindolyl derivatives in acute inflammation, pain and oxidative stress, Antiinflamm. Antiallergy Agents Med. Chem. 13 (2014) 165–173.
[38] R.J. Ruch, S.J. Cheng, J.E. Klaunig, Prevention of cytotoxicity and inhibition of intercellular communication by antioxidant catechins isolated from Chinese green tea, Carcinogenesis 10 (6) (1989) 1003–1008.
[39] J. Infante, P.L. Rosalen, J.G. Lazarini, M. Franchin, S.M. Alencar, Antioxidant and anti-Inflammatory activities of unexplored brazilian native fruits, PLoS One 11 (4) (2016) e0152974.
[40] T.C. Genaro-Mattos, Â.Q. Maurício, D. Rettori, A. Alonso, M. Hermes-Lima, Antioxidant activity of caffeic acid against iron-Induced free radical generation-A chemical approach, PLoS One 10 (6) (2015) e0129963.
[41] D. Isha, K. Nitesh, S.N. Manjula, P. Vipan, S.M. Manjunath, K.S.R. Pai, Preliminary evaluation of *in vitro* cytotoxicity and *in vivo* antitumor activity of Premna herbacea Roxb. in Ehrlich ascites carcinoma model and Dalton's lymphoma ascites model, Exp. Toxicol. Pathol. 65 (2013) 235–242.
[42] P. Thirusangu, V. Vigneshwaran, V.L. Ranganatha, B.R. Vijay Avin, S.A. Khanum, R. Mahmood, K. Jayashree, B.T. Prabhakar, A tumoural angiogenic gateway blocker, Benzophenone-1 B represses the HIF-1α nuclear translocation and its target gene activation against neoplastic progression, Biochem. Pharmacol. 125 (2017) 26–40.
[43] P. Thirusangu, V. Vigneshwaran, T. Prashanth, B.R. vijay avin, V.H., malojirao, H., rakesh, S.A., khanum, R., mahmood, B.T., prabhakar, BP-1T, an antiangiogenic benzophenone-thiazole pharmacophore, counteracts HIF-1 signalling through p53/MDM2-mediated HIF-1a proteasomal degradation, Angiogenesis 20 (2017) 55–71.